

advantage: a disadvantage because internal conversion is no longer the clean-cut tool it was once thought to be, and an advantage because conversion measurements now provide a means for determining additional nuclear information in the form of new nuclear matrix elements. The experimental data needed for the determination of such information are clearly (1) a knowledge of the multipole constituents of the transitions considered (e.g., from γ - γ correlation experiments), (2) a complete knowledge of the numerical factors appearing in the previous calculations, and (3) accurate experimental data on either internal-conversion coefficients, con-

version ratios or angular-correlation measurements involving the conversion electrons.²¹

ACKNOWLEDGMENTS

We thank Dr. M. Goldhaber for valuable suggestions, Dr. M. E. Rose for providing us with unpublished data on his internal-conversion calculations, and Dr. M. Deutsch and Dr. R. D. Hill for helpful discussions.

²¹ For a pure $M1$ transition the anisotropy in the conversion-electron correlation arises from the $d_{\frac{1}{2}}$ conversion electrons, the intensity of which is relatively unaffected by finite-size effects. However, the magnitude of the anisotropy is a function of the ratio of the amplitudes of the $d_{\frac{1}{2}}$ and $s_{\frac{1}{2}}$ matrix elements, and is therefore a function of λ .

Elastic Scattering of Protons by Beryllium*

FORREST S. MOZER†

Kellogg Radiation Laboratory, California Institute of Technology, Pasadena, California

(Received July 9, 1956)

Fifteen angular distributions and three excitation curves for the reaction $\text{Be}^9(p,p)$ have been obtained in the proton energy region between 200 and 3000 kev. Angular distributions for $\text{Be}^9(p,d)$ and $\text{Be}^9(p,\alpha)$ at 333 kev were also measured. The elastic scattering data have been analyzed and fitted in terms of the following states in B^{10} : an s -wave $J=1^-$ state near 330-kev proton bombarding energy; a p -wave $J=2^+$ state near 980 kev; an s -wave $J=2^-$ state near 998 kev; a p -wave $J=0^+$ state near 1084 kev; and an s -wave $J=2^-$ state near 1330 kev.

I. INTRODUCTION

THE states of B^{10} in the region above 6.585 Mev are conveniently reached by the reaction Be^9+p . Through this method of excitation, the study of the energy and angular distributions of the resultant deuterons, alpha particles, gamma rays, and elastically scattered protons, has yielded much information on the several states in this region.¹ This information has led to the recognition of energy levels in B^{10} at proton bombarding energies near 330, 995, 1085, and 2565 kev, and has suggested the existence of other states near 470 and 670 kev. While tentative spins, parities, and isotopic spins of these states have been obtained from partial analysis of the scattering and reaction data, each of the known states exhibited at least one property contradicting the tentative assignments thus obtained.

The 330-kev state (6.89 Mev-excitation in B^{10}), assumed to be $J=1$ and to be formed by s -wave protons, appeared to have $T=0$ because it was observed to decay by deuteron and alpha-particle emission. On the other hand, the strong electric dipole gamma-ray transitions to the low excited states of B^{10} suggested $T=1$ for the

330-kev state, since electric dipole transitions between two isotopic spin zero states are highly forbidden.² Thus, if the 330-kev state was formed by s -wave protons, it possessed the largest isotopic spin impurity of any known level in light nuclei.

The 995-kev level (7.48-Mev excitation in B^{10}), presumed to be a 2^- state formed predominantly by s -wave protons with a small d -wave admixture, exhibited the same isotopic spin difficulties as the 330-kev level since it produced both deuterons and alpha particles yet had an electric dipole gamma-ray width of about 10 ev. Furthermore, the existence of an electric octopole transition 1000 times larger than the single-particle model limit was suggested by the angular correlation of internal conversion pairs emitted in the ground state transition. The facts that below resonance the cascade gamma-ray yield could not be fit by a Breit-Wigner curve, and that the deuteron and alpha reaction products peaked about 50 kev below the gamma rays, were not understood.

The narrow 1085-kev resonance had been incompletely studied, but the smallness of the elastic scattering anomaly along with the cascade gamma transitions suggested a total spin of zero for the state.

The region between 1085 and 2565 kev was unobserved in the elastic scattering process. It was for this

* Supported in part by the joint program of the Office of Naval Research and the U. S. Atomic Energy Commission.

† Lockheed Leadership Fellow, 1955-1956.

¹ For a complete discussion of the states in B^{10} along with references on the data discussed, see F. Ajzenberg and T. Lauritsen, *Revs. Modern Phys.* **27**, 77 (1955).

² W. M. MacDonald, *Phys. Rev.* **98**, 60 (1955).

reason, along with the desire to clarify the properties of the 995- and 330-keV states, that the present experiment was undertaken.

II. EXPERIMENTAL APPARATUS AND TECHNIQUES

Incident proton beams of from 0.01 to 20 microamperes, monoenergetic to better than 0.1%, were obtained by passing the output of a 1.8-MeV electrostatic generator through a cylindrical electrostatic analyzer. Particles elastically scattered in the target were analyzed by a high-resolution double-focusing magnetic spectrometer³ which was mounted to allow a continuously variable scattering angle from 0 to 160 degrees with respect to the incident beam direction. The resultant magnetically analyzed particles were counted by means of a cesium iodide, thallium-activated, scintillation crystal backed by a DuMont 6291 photomultiplier, standard preamplifier, amplifier, and scaling circuits.

The incident particle electrostatic analyzer was calibrated by comparison with the 873- and 1372-keV resonances in $F^{19}(p,\alpha\gamma)$. With this energy scale established, the magnetic spectrometer was calibrated by observation of protons elastically scattered from copper. Both the electrostatic analyzer and magnetic spectrometer calibrations were found to be independent of energy and scattering angle to better than one part in six hundred over the entire range of energies and angles used in the present experiment.

All cross sections have been normalized to the assumed Rutherford cross section for the elastic scattering of protons by copper. In the course of the experiment, the elastic scattering of protons by thick copper targets prepared and polished by different methods was studied, and it was found that poorly polished or roughly machined targets produced a smaller yield of particles per unit momentum interval than did evaporated or highly polished targets. As a result of experiments on different types of scratched target surfaces, it has been concluded that this yield loss results from protons that enter the target near the bottom of a scratch, react, and emerge through the smooth part of the target after traversing a distance the order of the scratch depth in the target. Since this distance is large compared to the distance of traversal of protons in a smooth target, those protons incident near the bottom of a scratch emerge with a momentum too small to allow them to traverse the magnetic spectrometer and be counted; hence a reduced yield is obtained. If this effect is to be avoided, the average scratch depth must be small compared to the normal depth of penetration of the protons that emerge with the proper momentum to be counted.

Excitation curves for the ratio of the experimental elastic scattering differential cross section to the calculated Rutherford scattering cross section for protons on beryllium have been measured in the energy region between 200 and 1700 keV at center-of-mass angles corresponding to the zeros of the first and second Legendre polynomials and at the largest obtainable scattering angle, $160^\circ 59'$, (Fig. 1), and from 1650 to 3000 keV at $146^\circ 18'$ (Fig. 2). Additional detailed excitation curves near the 1084-keV resonance have also been obtained (Figs. 3 and 4), as well as fifteen angular distributions at selected energies between 220 and 1664 keV (Figs. 5 through 19). In addition to these elastic scattering data, the $Be^9(p,d)$ and $Be^9(p,\alpha)$ reaction angular distributions were measured at the 330-keV resonance (Figs. 20 and 21) to test the validity of the assumption that this resonance is formed by *s*-wave protons.

These reaction-product angular distributions as well as the excitation curves near the 1084-keV resonance and the forward-angle cross-section measurements of Figs. 10, 12, and 14 were obtained by using thin targets of beryllium and calculating cross sections from the equations of Snyder, Rubin, Fowler, and Lauritsen.³ For the studies near 1084 keV, a 0.7-keV layer of beryllium evaporated on a 5-keV unsupported nickel foil served as the target. The reaction cross-section studies were made by using a 4.5-keV (to 1-MeV protons) beryllium layer evaporated on a chromium-plated thick brass backing. The elastic scattering thin-target studies were carried out with targets of unsupported beryllium foils between 10 and 30 keV thick to 1-MeV protons.

The remainder of the excitation curves and angular distributions were obtained by using one-eighth inch thick beryllium disks as targets and separating the resultant particles produced in a thin lamina at any desired depth in the target by means of the high resolution of the resultant particle magnetic analyzer. Cross sections were calculated from these thick-target data by means of equations given by Snyder *et al.*³ The stopping cross section of protons in beryllium that enters into these equations is given by Bader, Pixley, Mozer, and Whaling.⁴

The total probable error of these elastic scattering determinations averaged 7%, the main contribution coming from the 4% uncertainty of the stopping cross section for protons in beryllium and copper, with lesser contributions arising from statistical counting fluctuations, background subtractions, corrections for the dead time of the counting equipment, current integrator uncertainties, and uncertainties in the electrostatic and magnetic analyzer energy calibrations and the magnetic analyzer angle setting.

³ Snyder, Rubin, Fowler, and Lauritsen, *Rev. Sci. Instr.* **21**, 852 (1950).

⁴ Bader, Pixley, Mozer, and Whaling, *Phys. Rev.* **103**, 32 (1956).

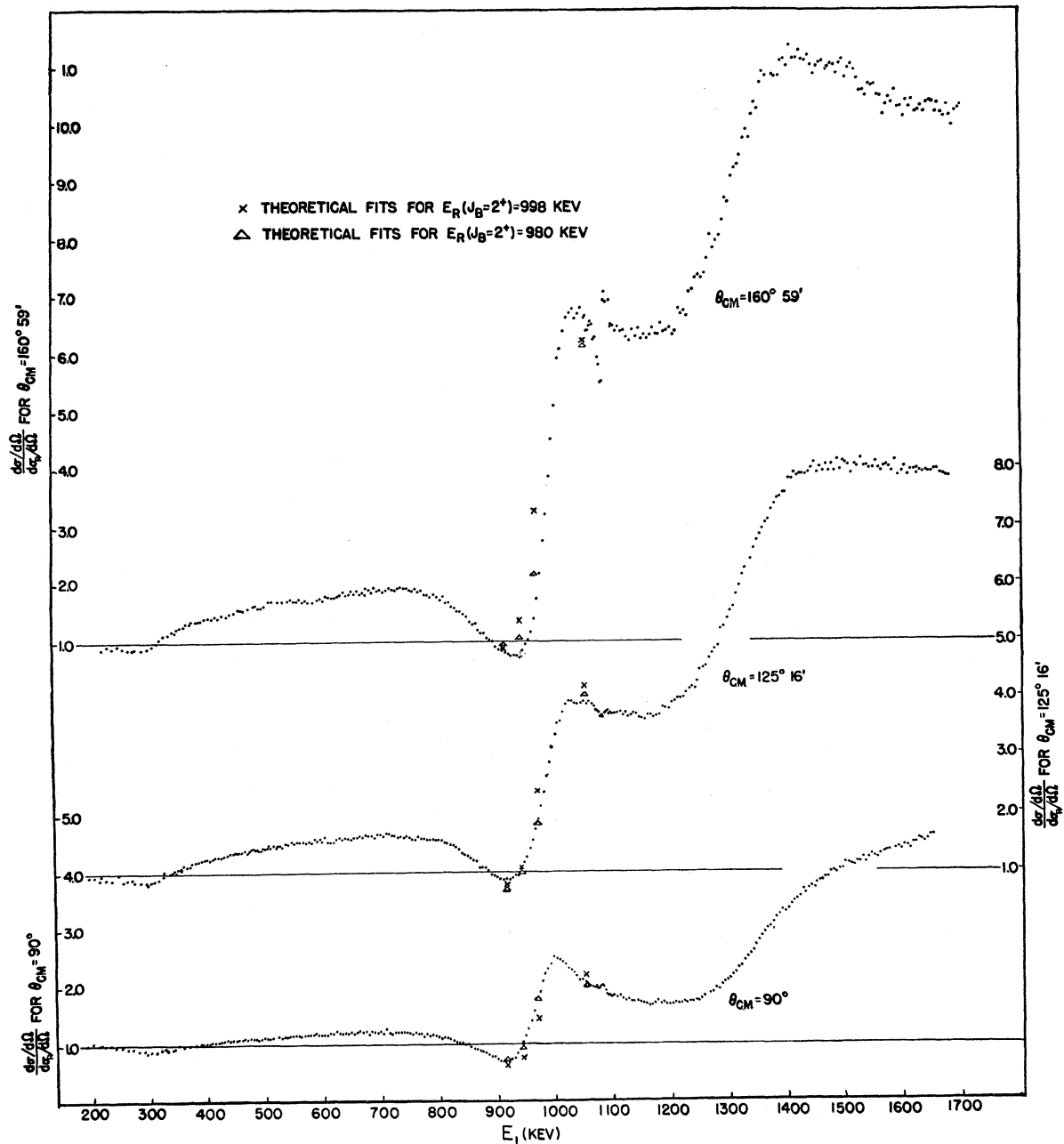


FIG. 1. The elastic scattering of protons by beryllium.

III. THEORETICAL ANALYSIS OF THE ELASTIC SCATTERING DATA

The general methods of analysis of elastic scattering data have been covered by Christy.⁵ Hence, only those specific points concerning the analysis procedure that apply to the case of the elastic scattering of protons by beryllium will be discussed.

⁵ R. F. Christy, Report on Amsterdam Conference, 1956; Physica (to be published). The notation used in the present paper follows that adopted in this reference.

The theoretical elastic scattering cross section is composed of the sum of squares of coherently interfering amplitudes of two types. The first type is the Rutherford scattering amplitude f_c , and is given by

$$f_c = R^{\frac{1}{2}} e^{i\zeta}, \quad (1)$$

where $R = (ZZ'e^2/2\mu v^2)^2 \csc^4(\frac{1}{2}\theta)$, $\zeta = -\alpha \ln \sin^2(\frac{1}{2}\theta)$, and $\alpha = ZZ'e^2/\hbar v$.

The second type of amplitude is the compound nuclear amplitude which is a product of three terms:

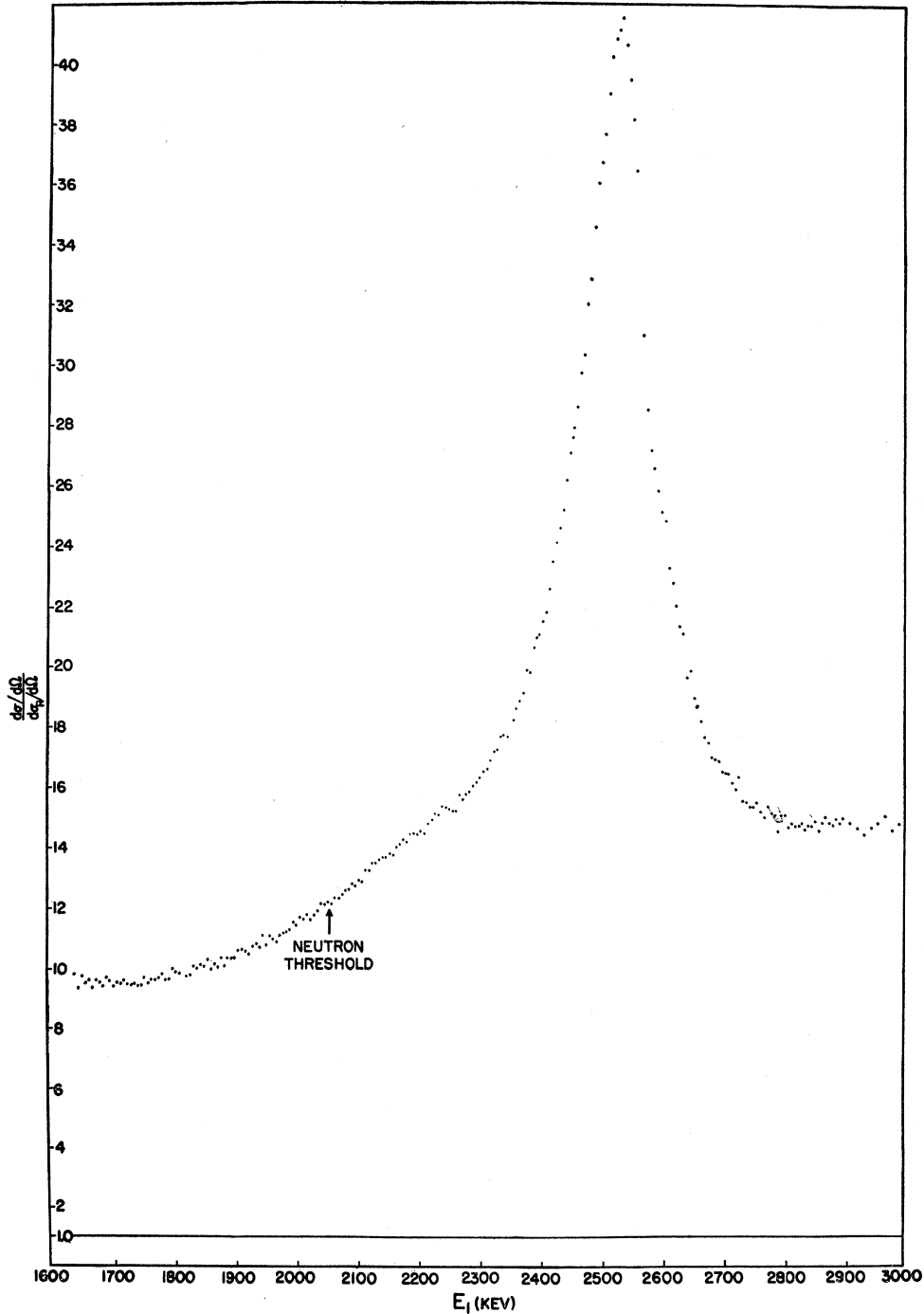


FIG. 2. The elastic scattering of protons by beryllium at $\theta_{c.m.} = 146^\circ 18'$.

two Clebsch-Gordan coefficients that represent the probability amplitudes for formation and decay of the compound nucleus through a particular combination of channel spins and orbital angular momenta, an angle-dependent factor given by the spherical harmonic $Y_{l', m'}$, and a group of constants and phase-shift-dependent terms that will be denoted by $f(J_B; J_{ch}; J_{ch}'; l; l')$

where J_B is the total spin of the compound state, J_{ch} is a channel spin, l , is an orbital angular momentum, and primed quantities refer to reaction products. The term $f(J_B; J_{ch}; J_{ch}'; l; l')$ is given by

$$f(J_B; J_{ch}; J_{ch}'; l; l') = (\pi^{1/2} i / k) i^{(l-l')} \times (2l+1)^{1/2} e^{i(\eta_l + \eta_{l'} - 2\eta_0)} f_{sc}, \quad (2)$$

where

$$e^{i(\eta_l - \gamma_0)} = \frac{(1+i\alpha) \cdots (l+i\alpha)}{(1+\alpha^2)^{\frac{1}{2}} \cdots (l^2+\alpha^2)^{\frac{1}{2}}}$$

Throughout the analysis it is assumed that potential scattering and nonresonant reaction cross sections occur only in the pure *s*-wave channels. Hence, for all higher orbital angular momenta ($l \geq 1$) a satisfactory form of the scattering amplitude f_{sc} is

$$f_{sc} = \alpha(J_B; J_{ch}; l) \alpha(J_B; J_{ch}'; l') \frac{(\Gamma_{pl} \Gamma_{pl'})^{\frac{1}{2}}}{\Gamma} (e^{2i\delta} - 1), \quad (3)$$

where Γ_{pl} and Γ are, respectively, the proton width for *l*-wave particles and the total width. The resonance phase shift δ is given by

$$\cot \delta = (E_R - E) / (\frac{1}{2}\Gamma). \quad (4)$$

The channel spin amplitude $\alpha(J_B; J_{ch}; l)$ is the nuclear probability amplitude of forming the given J_B from the orbital angular momentum *l* and the channel spin J_{ch} , and is related to the method of nuclear coupling of the intrinsic angular momenta of the target and bombarding particle with their relative orbital angular momentum. From its definition it follows that

$$\alpha(J_B; J_{ch}; l) = 0 \quad \text{unless} \quad J_B = J_{ch} + l \quad (5)$$

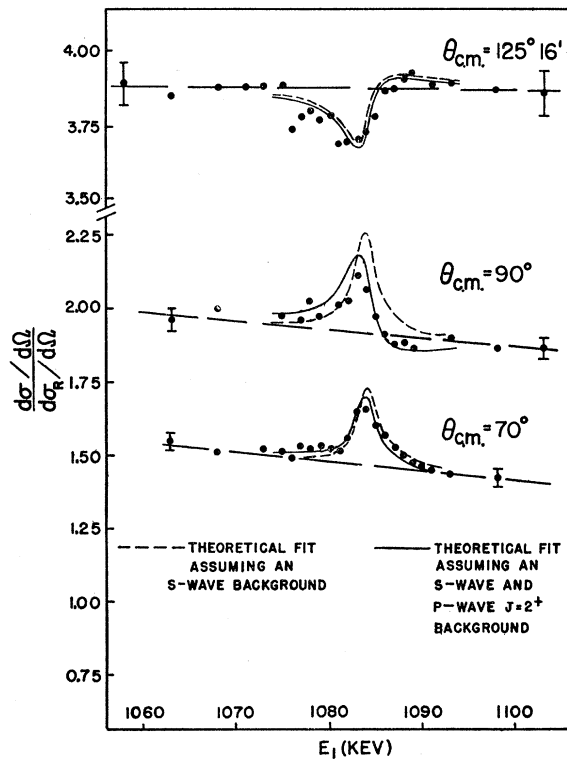


FIG. 3. The elastic scattering of protons by beryllium. (Note suppressed zero of ordinate scale.)

and

$$\sum_{J_{ch}} [\alpha(J_B; J_{ch}; l)]^2 = 1.$$

For pure *s*-wave scattering, the scattering amplitude f_{sc} should include the possibility of potential scattering and nonresonant reaction cross sections. Since there is no *a priori* energy variation of these quantities, the pure *s*-wave f_{sc} is left as an unknown to be determined by obtaining the best theoretical fit of the experimental data. Writing

$$f_{sc}(J_B) = f(J_B) + ig(J_B) - 1, \quad (6)$$

the four unknowns $f(1)$, $g(1)$, $f(2)$, and $g(2)$ are thus introduced into the theoretical elastic scattering equations.

Since the validity of an analysis depends on obtaining good fits to the experimental data with reasonable choices of the above four parameters, and since the above four parameters contain all the information about *s*-wave resonances that can be deduced in the analysis procedure, a study of the energy variations of these fitting parameters must be made to determine their reasonableness and to deduce from them the *s*-wave resonance parameters. This procedure is carried out by comparing $f(1)$, $g(1)$, $f(2)$, and $g(2)$ with some standard theoretical form for f_{sc} . Such a form, for the particular case of one isolated *s*-wave resonance whose total

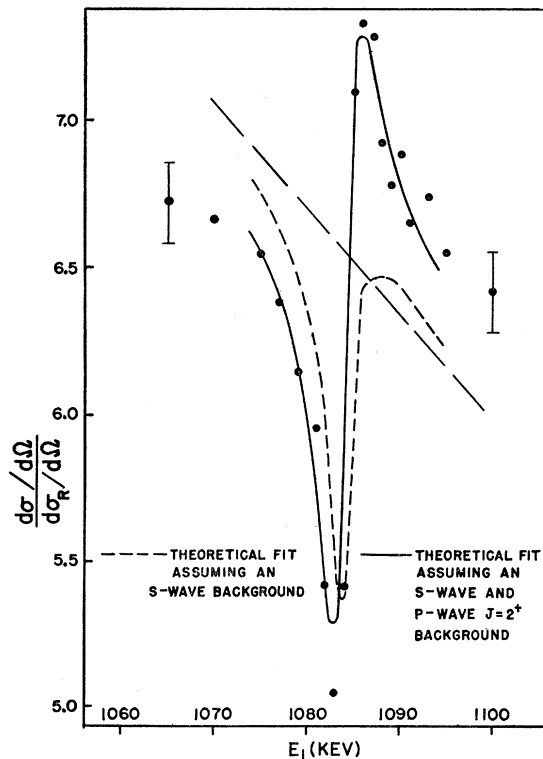


FIG. 4. The elastic scattering of protons by beryllium at $\theta_{c.m.} = 160^\circ 59'$. (Note suppressed zero of ordinate scale.)

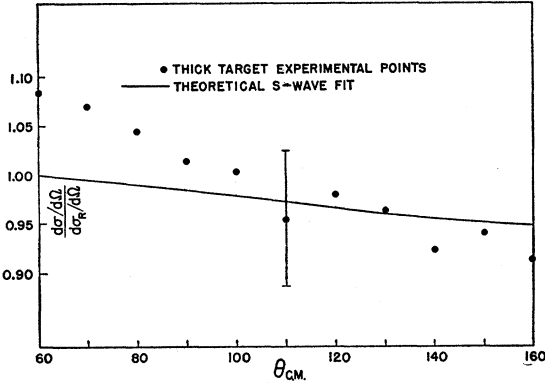


FIG. 5. The elastic scattering of protons by beryllium at $E_1=220$ kev. (Note suppressed zero of ordinate scale.)

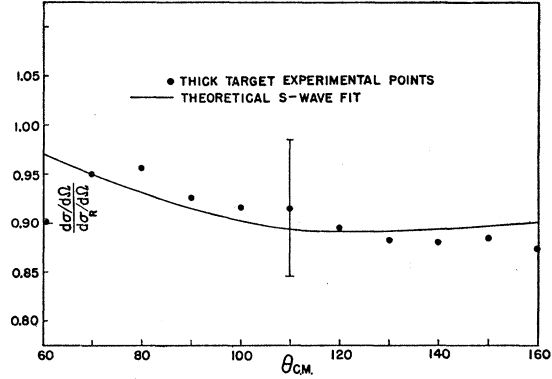


FIG. 6. The elastic scattering of protons by beryllium at $E_1=273$ kev. (Note suppressed zero of ordinate scale.)

reaction cross section adds incoherently to a constant background reaction cross section is

$$f_{sc} = e^{2i\phi} \frac{\Gamma_p}{\Gamma} (e^{2i\delta} - 1) + (1 - \beta) e^{2i\phi} - 1. \quad (7)$$

From the conservation of particles, the constant background reaction cross section can be obtained as

$$\sigma_{\text{reaction}} = \pi \lambda^2 \omega \beta (2 - \beta). \quad (8)$$

Thus β is related to the nonresonant reaction cross section and ϕ is an elastic scattering potential phase shift since its presence affects the elastic scattering but not the reactions.

For later comparisons of $f(1)$, $g(1)$, $f(2)$, and $g(2)$ with Eq. (7), a geometric interpretation of β and ϕ is obtained by plotting $f_{sc} + 1$ in the complex plane as in Fig. 22. As the proton energy is increased through the region of an s -wave resonance, 2δ increases through 2π and $f_{sc} + 1$ traces out a resonance circle of radius Γ_p/Γ that lies entirely within the unit circle. This resonance circle is displaced from the real axis by an angular amount 2ϕ and from tangency with the unit circle by the amount β . A plot of the fitting parameters $f(J_B)$ versus $g(J_B)$ must exhibit these same properties in the region of a resonance, the resonance parameters being determined by the size and location of the resonance circle.

To be more accurate, it should be pointed out that what has been drawn as and referred to as resonance circles above will tend to be more nearly elliptical in any actual example. This follows from the fact that because of barrier penetration, Γ_p/Γ is a monotonically increasing function of energy for protons on Be⁹. Hence the radius of the resonance circle increases as it is traversed, the result being a more nearly elliptical than circular motion.

The simplest theoretical elastic scattering equation is obtained from the assumption of s -wave formation and decay of the compound nucleus. Hence, unless there are existing experimental arguments for believing that the

states of interest are not formed by s waves, the simplest analysis is obtained by attempting to fit the experimental angular distributions with the pure s -wave theoretical cross-section equation. This was the first method applied in the analysis of the elastic scattering of protons by beryllium.

The four parameters $f(1)$, $g(1)$, $f(2)$, and $g(2)$ combine in the pure s -wave theoretical elastic scattering equation into three unknowns,

$$\begin{aligned} X &= \frac{3}{8}f(1) + \frac{5}{8}f(2), \\ Y &= \frac{3}{8}g(1) + \frac{5}{8}g(2), \\ U &= 1 - \frac{3}{8}\{[f(1)]^2 + [g(1)]^2\} - \frac{5}{8}\{[f(2)]^2 + [g(2)]^2\} \\ &= \sigma_{\text{reaction}}/\pi\lambda^2. \end{aligned} \quad (9)$$

Since the detailed fitting of the experimental angular distributions happened to be insensitive to the choice of U , it was calculated from the known reaction cross section.⁶ Pure s -wave fits on all angular distributions were then made with a theoretical equation involving only the two undetermined parameters X and Y . In certain energy regions, the pure s -wave analysis failed to meet the double requirement of fitting the experimental data with reasonable fitting parameters. In these regions, other theoretical cross-section equations were used in attempting to obtain a fit of the data. These procedures will be covered more thoroughly in the following discussion of the properties of the states of B¹⁰ as determined from the theoretical analysis of Be⁹(p, p).

A summary of the properties of the states of B¹⁰ in the energy region covered by the present experiment is given in Table I. The following discussion concerns the methods of theoretical deduction of these properties.

The structure of the elastic scattering curves between 200 and 700 kev indicates the presence of a broad resonance anomaly near 330 kev. From its

⁶ The data of Thomas, Rubin, Fowler, and Lauritsen, Phys. Rev. 75, 1612 (1949), increased by 8% to agree with the data of Figs. 20 and 21, have been used in these calculations. The cross section is assumed to be isotropic over the low-energy region.

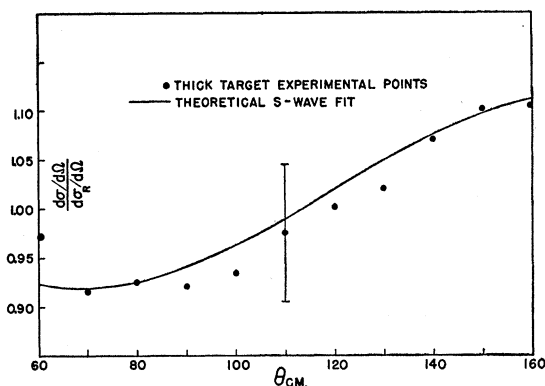


FIG. 7. The elastic scattering of protons by beryllium at $E_1=329$ kev. (Note suppressed zero of ordinate scale.)

large width and the presence of an interference anomaly at all angles of observation, the compound nuclear state appears to be formed by s waves. Furthermore, the decrease of the ratio to Rutherford at all angles below resonance is consistent only with s -wave formation of the compound state, if higher than s -wave potential scattering is not present. Thus, the first procedure involved in the low-energy analysis was an attempt to fit the low-energy angular distributions by a pure s -wave theoretical cross-section equation. Results of this procedure are shown in Figs. 5 through 11. In these figures the 7% error indicated on the 110-degree data serves to orient the eye to the accuracy within which the theoretical expressions approximate the experimental data.

In the region between 220 and 776 kev, the pure s -wave theoretical equation is seen to agree with the experimental data to within experimental error. From the plot of the X versus Y obtained in the above analysis and illustrated in the scattering amplitude diagram of Fig. 23, it is seen that the fitting parameters X and Y exhibit the proper resonance behavior expected of an s -wave state. This fact along with the angular isotropy of reaction products (Figs. 20 and 21) leads

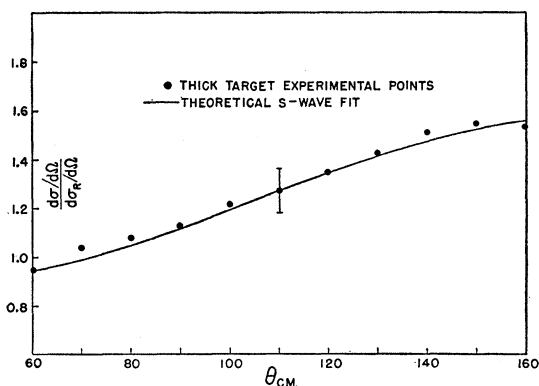


FIG. 8. The elastic scattering of protons by beryllium at $E_1=439$ kev. (Note suppressed zero of ordinate scale.)

to the conclusion that the 330-kev state has odd parity and a total spin of one or two.

From the tangency of the resonance ellipse and unit circle in the scattering amplitude diagram of Fig. 23, the quantity β of Eq. (7) is zero, and there is no nonresonant reaction cross section in the s -wave channels at the lowest energies. From the fact that the center of the resonance circle is near the real axis, the potential scattering phase shift is nearly zero. Both of these effects are to be expected at sufficiently low energies.

Under the assumptions that the potential and nonresonant phase shifts are constant over the region of the resonance, it is seen from Eqs. (6), (7), and (9), that the radius of the resonance ellipse is given by $\omega\Gamma_p/\Gamma$, where

$$\begin{aligned} \omega &= \frac{3}{8} \quad \text{for } J_B=1 \\ &= \frac{5}{8} \quad \text{for } J_B=2. \end{aligned}$$

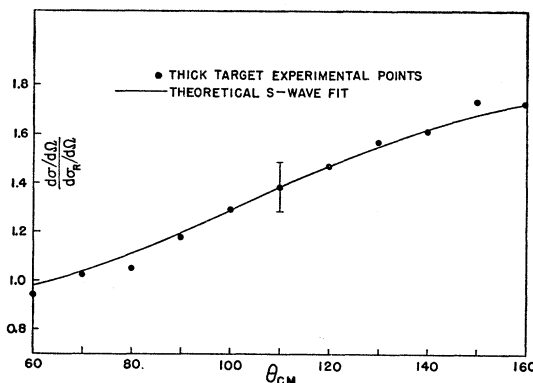


FIG. 9. The elastic scattering of protons by beryllium at $E_1=557$ kev. (Note suppressed zero of ordinate scale.)

Since the radius and Γ_p/Γ vary with energy because of barrier penetration, it is required in discussing partial or total widths to specify the energy to which these quantities refer. From the radius of the resonance ellipse at 330 kev the partial proton width at that energy is given by

$$\begin{aligned} \Gamma_p/\Gamma &= 0.18 \quad \text{if } J_B=2 \\ &= 0.30 \quad \text{if } J_B=1. \end{aligned}$$

It must be emphasized that these values of partial proton width are only accurate to about a factor of two. This arises from the fact that the theoretical equations yield values for $[(d\sigma/d\Omega)/(d\sigma_R/d\Omega)]-1$, which in the energy region under consideration is a number of the order of 0.1. A five percent decrease in cross section halves this number and thereby changes the fitting parameters and the radius of the resonance ellipse considerably.

The total width of the 330-kev state may in principle, be determined by the energy variation of the low-energy region of the scattering amplitude diagram of

Fig. 23. However, such a determination requires knowledge of the energy variation of the resonant phase shift which in turn depends on the level shift $\Delta_\lambda(E)$.⁷ Since $\Delta_\lambda(E)$ involves the reduced widths for various types of emission, it follows that the elastic scattering data does not yield sufficient information to deduce the total width of the 330-keV state. Recourse must thus be made to the known $\text{Be}^9(p,d)$ and $\text{Be}^9(p,\alpha)$ reaction cross-section data.⁶

The conclusion reached from the detailed fitting of the reaction cross-section data by the one-level formula involving the energy variation of the level shift $\Delta_\lambda(E)$ is that no total width less than the single-particle limit will yield the correct cross sections at resonance and the large contribution above resonance indicated by the data of Thomas, Rubin, Fowler, and Lauritsen. Thus, a background reaction cross section presumably exists in other than the s -wave channels, since the scattering amplitude diagram resonance ellipse is

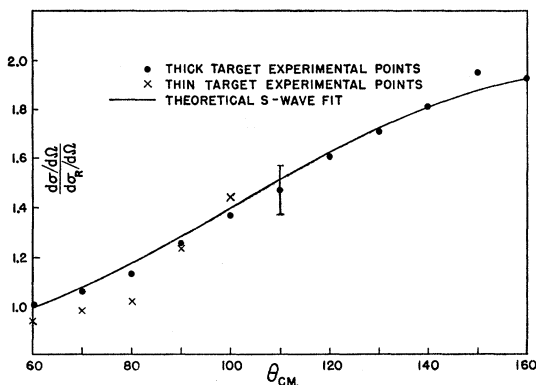


FIG. 10. The elastic scattering of protons by beryllium at $E_1=668$ keV. (Note suppressed zero of ordinate scale.)

tangent to the unit circle. The determination of the total and partial widths being dependent on the nature and amount of this background, it is impossible without further detailed investigations in this energy region to determine partial widths for the 330-keV state.

However, some general conclusions do follow from the gross features of the reaction cross-section curves. The total width and the reduced partial widths of the 330-keV state must be quite large. The best fit of the one-level formula to the experimental data with a particular choice of background subtraction is obtained for a proton reduced width that is about 50% of the single-particle limit of 5.7 MeV, a deuteron reduced width that is about 40% of the single-particle limit of 1.9 MeV, and a reduced alpha width of about 5% of the single-particle limit of 1.7 MeV. Various methods of background subtraction can vary these values by factors as large as two or three, but it must generally be true that very large proton and deuteron reduced

⁷ E. Wigner and L. Eisenbud, Phys. Rev. **72**, 29 (1947).

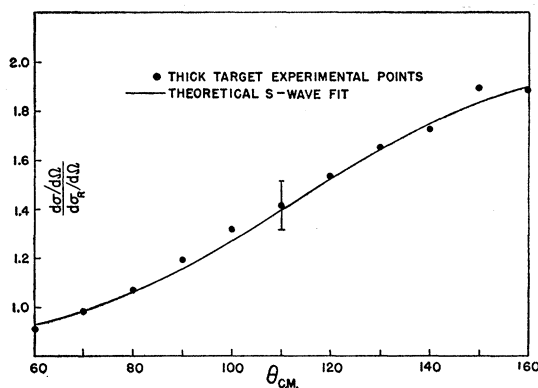


FIG. 11. The elastic scattering of protons by beryllium at $E_1=776$ keV. (Note suppressed zero of ordinate scale.)

widths and a somewhat smaller alpha reduced width are required to explain the experimental data.

The first step in the analysis of the angular distributions between 776 and 1664 keV was to attempt a fitting by the pure s -wave theoretical cross-section equation in the manner previously indicated. Results of this fitting procedure are shown in Figs. 12 through 19, where the 7% error on the 110° data at all energies again serves to orient the eye to the accuracy with which the theoretical equation fits the experimental data.

The discrepancy between the theoretical fits and the experimental data being greater than the probable error of the experimental determinations at many angles in the majority of the angular distributions, the validity of the pure s -wave analysis was highly suspect. Further doubt was cast on its validity near 1 MeV by observing that the energy variation of the scattering-amplitude diagram plot of X versus Y (see Fig. 23) does not exhibit the counter-clockwise rotation expected of a resonant type behavior. Thus the pure s -wave analysis could satisfy neither of the two requirements on a valid theoretical analysis, and the situation near 1 MeV was investigated more thoroughly.

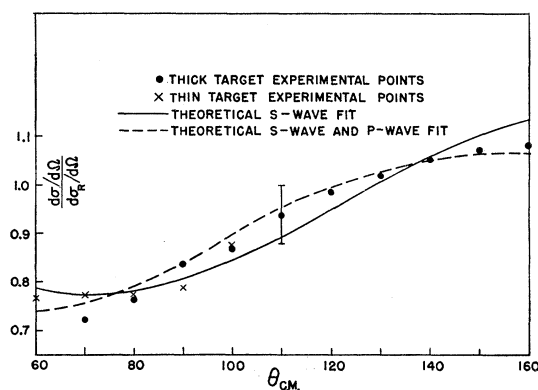


FIG. 12. The elastic scattering of protons by beryllium at $E_1=887$ keV. (Note suppressed zero of ordinate scale.)

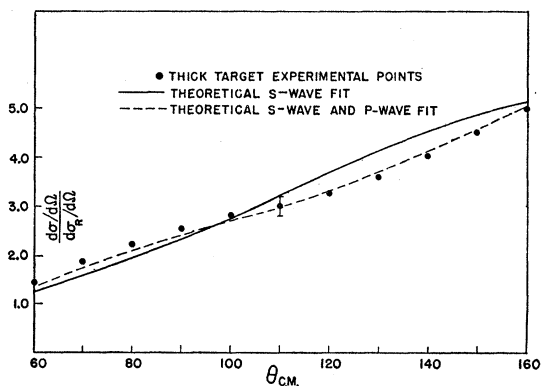


Fig. 13. The elastic scattering of protons by beryllium at $E_1=998$ kev. (Note suppressed zero of ordinate scale.)

Because the excitation curves near 1 Mev exhibit interference minima at all angles of observation, it seemed desirable to retain the assumption that the 1-Mev state is formed predominantly by s waves. A hint of a possible modification of the pure s -wave equation was supplied by the ground state gamma-ray transition angular distribution which is of the form $1 + (0.10 \pm 0.03) \sin^2\theta$.⁸ This nonisotropy is explainable by the assumption of a small contribution to the formation of the state by d -wave protons. And thus, a second attempt at analysis of the angular distributions was made by allowing for d -wave formation and decay. Since the theoretical cross-section equation expressing s -wave and d -wave formation or decay of the compound nucleus contains seven unknowns, a unique analysis of the experimental data was nearly impossible. However, qualitative consideration of the theoretical equation was enough to show that the inclusion of d -wave protons does not improve the fitting of the experimental data for any reasonable set of assumptions on the seven unknowns.

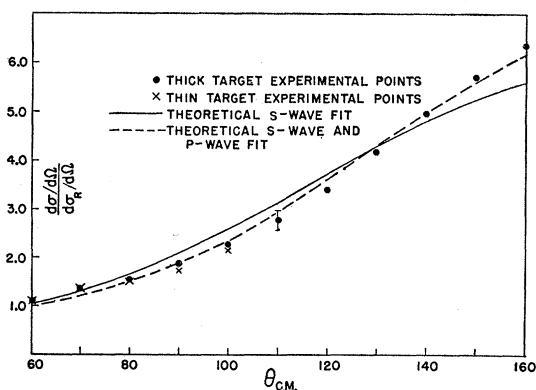


Fig. 14. The elastic scattering of protons by beryllium at $E_1=1108$ kev. (Note suppressed zero of ordinate scale.)

⁸ E. P. Paul and H. E. Gove, Proc. Roy. Soc. (Canada) 47, 145(A) (1953).

Thus, the theoretical analysis near 1 Mev was not aided by the addition of d waves, and it became necessary to look to sources other than the gamma-ray angular distribution data for clues to assumptions that would enable a fit of this data. A source of such a clue was obtained from a study of the narrow 1084-kev level, since the analysis in this region is sensitive to the assumed background which arises in part from the 1-Mev broad level.

The gross features of the thin-target excitation curves near 1084 kev illustrated in Figs. 3 and 4 supply some insight into the spin and parity of the compound nuclear state. Under the experimentally verified assumption that $\Gamma_p/\Gamma=1$, the smallness of the anomaly at the forward angles is consistent only with a $J_B=0$ state in B^{10} . The determination of the parity of the state rests on the magnitudes of the interference terms at the zeros of $P_1(\cos\theta)$ and $P_2(\cos\theta)$. At 90° there is practically no interference as is seen by the symmetry of the anomaly about the resonance energy, while at $125^\circ 16'$, the resonance anomaly is composed almost entirely of interference terms. While such a behavior may not be inconsistent with d -wave formation of the compound state if one assumes the background to be composed in a large measure of other than s -wave amplitudes, the simplest assumption is that the 1084 state is formed by p waves, hence $J_B=0^+$.

With the assumptions that $J_B=0^+$, that there is no potential scattering or nonresonance reaction cross section in the p -wave channels, and that only s -wave amplitudes are present in the background, the theoretical fits illustrated in Figs. 3 and 4 are obtained. Since these assumptions are not sufficient to explain the anomaly at the back angle, additional amplitudes must be introduced into the theoretical equation.

An obvious extension of the analysis is to include the supposed d -wave present in the formation of the 1-Mev state. However, 2^- d -wave amplitudes do not interfere with the 0^+ p -wave amplitudes and thus, some other assumption must be advanced.

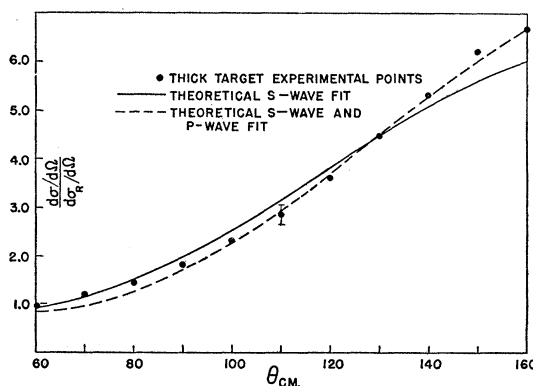


Fig. 15. The elastic scattering of protons by beryllium at $E_1=1220$ kev. (Note suppressed zero of ordinate scale.)

A logical approach is to include all p -wave amplitudes in the background, then all d -wave amplitudes, etc., until the background contains enough variables to fit the experimental data. Of the possible p -wave amplitudes, only those leading to a 2^+ state in B^{10} are considered plausible in the background, because the 1^+ and 3^+ states do not interfere with a 0^+ state, and a 0^+ state in the background will not produce the deuterons and alpha particles that must be present in this energy region to account for the $\cos\theta$ term in the deuteron and alpha angular distributions near 1 Mev.⁹ Thus, a 2^+ p -wave state is included in the background, and the new parameters $\alpha_1^2\Gamma_{p2}/\Gamma_2$ and $\cos\delta_2$ are inserted into the analysis, where α_1 is the channel-spin-dependent part of the probability amplitude for the formation of a $J_B=2^+$ state from p -wave protons through channel spin one, Γ_{p2} and Γ_2 are, respectively, the partial proton and total width of the 2^+ state, and δ_2 is its resonance phase.

With a 0^+ resonant state superimposed on a background made up of 2^- and 1^- s -wave and 2^+ p -wave amplitudes, the theoretical fits of the experimental data shown in Figs. 3 and 4 are obtained with the following choices of variable parameters:

$$f(1) = -0.4, \quad g(1) = -0.9, \\ \alpha_1^2\Gamma_{p2}/\Gamma_2 = 0.9, \quad \cos\delta_2 = -0.918.$$

As a further assumption in the following discussions, it is assumed that $\alpha_1^2=1$ and $\Gamma_{p2}/\Gamma_2=0.9$, values that are accurate to about 10% if the 1084-keV analysis is correct.

Since the presence of a 2^+ p -wave state in the background enables a quantitative fit of the experimental data at the 1084-keV narrow resonance, such an assumption must be tested on the elastic scattering angular distributions and excitation curves in the neighborhood of 1 Mev. With the parameters obtained from the 1084-keV fit, the theoretical cross-section formula expressing the presence of a 2^+ p -wave state and an arbitrary amount of s wave contains, as

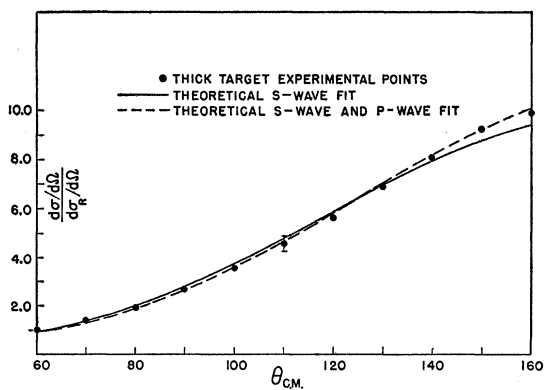


FIG. 16. The elastic scattering of protons by beryllium at $E_1=1330$ keV. (Note suppressed zero of ordinate scale.)

⁹ Neuendorffer, Inglis, and Hanna, Phys. Rev. 82, 75 (1951).

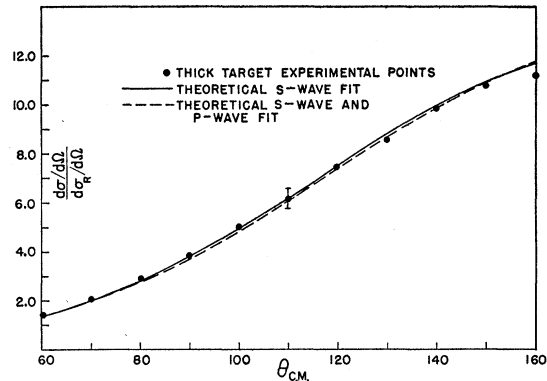


FIG. 17. The elastic scattering of protons by beryllium at $E_1=1440$ keV. (Note suppressed zero of ordinate scale.)

unknowns, the resonance energy of the 2^+ state in addition to $f(1)$, $g(1)$, $f(2)$, and $g(2)$. Thus, the presence of a p -wave state breaks up the degeneracy in s -wave amplitudes and detailed fitting enables the determination of the variation of both the $J_B=2^-$ and $J_B=1^-$ s -wave scattering amplitudes, rather than a combination of them as was obtained with the pure s -wave equation.

The resonance energy of the 2^+ state was determined by fitting the excitation curves of Fig. 1 for the two assumptions $E_R=998$ keV and $E_R=980$ keV, assuming the s -wave scattering amplitudes given in Fig. 23. From the results of this fitting procedure and the reasonableness of the fitting parameters assumed in the analysis, the resonance energy of the 2^+ state is 980 keV to within about 10 keV. The width of the 2^+ p -wave state at 980 keV as determined from its resonance energy and $\cos\delta_2$ at 1084 keV, neglecting effects of the level shift $\Delta_\lambda(E)$, is 90 keV. This corresponds to a reduced width that is about 7% of the single-particle limit.

The next step in the analysis was the fitting of the angular distributions between 887 and 1664 keV with the theoretical s -wave and p -wave $J_B=2^+$ cross-section

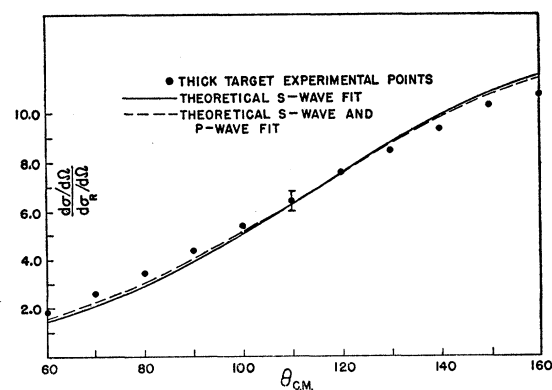


FIG. 18. The elastic scattering of protons by beryllium at $E_1=1552$ keV. (Note suppressed zero of ordinate scale.)

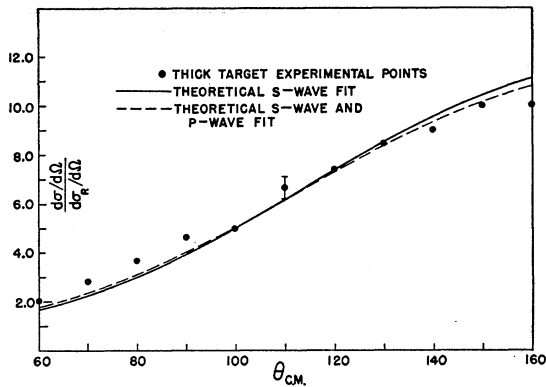


FIG. 19. The elastic scattering of protons by beryllium at $E_1=1664$ kev. (Note suppressed zero of ordinate scale.)

equation. The results of this process are shown in Figs. 12 through 19. At all energies the addition of the p -wave state is seen to improve the character of agreement between experiment and theory.

The resulting scattering amplitude diagram plots of $f(1)$ versus $g(1)$ and $f(2)$ versus $g(2)$ are shown in Fig. 23. The general behavior of the energy variation of $f(2)$ versus $g(2)$ indicates two counterclockwise resonance circles corresponding to two $J_B=2^-$ states in B^{10} near energies of 998 kev and 1330 kev. The energy variation of $f(1)$ versus $g(1)$ shows what may be interpreted as the tail of the 330-kev resonance along with a potential phase shift and the hint of what might be a higher energy s -wave $J=1^-$ resonance that causes the scattering amplitude diagram plot to reverse direction and start in a counterclockwise circle at the high energies. These behaviors might be expected in view of Lane's prediction of four s -wave states, two $J_B=1^-$ and two $J_B=2^-$, in this energy region.¹⁰

The validity of the fitting procedure being assumed by virtue of its satisfying the double requirement of

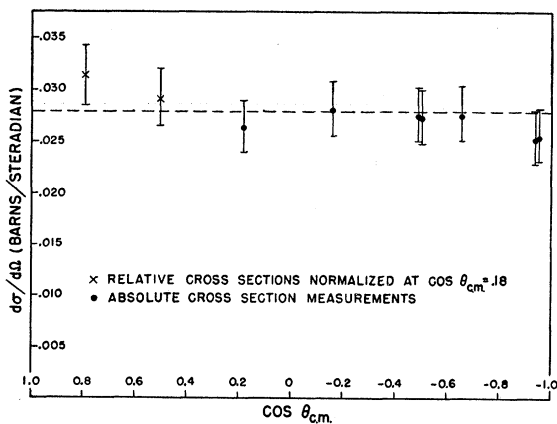


FIG. 20. The differential cross section for $Be^9(p,\alpha)$ at $E_1=333$ kev. (Note suppressed zero of ordinate scale.)

¹⁰ A. M. Lane, Atomic Energy Research Establishment, Harwell Report, T/R 1289, 1954 (unpublished).

fitting the data with proper energy-varying parameters, the scattering amplitude diagram must be studied in greater detail to determine the properties of the potential phase shifts in the $J_B=1^-$ channel and the compound nuclear states in the $J_B=2^-$ channel.

From a simple model of hard-sphere scattering in the absence of a Coulomb potential, Wigner¹¹ derives the inequality

$$d\phi/dk > -R \quad (10)$$

from the law of causality that the scattered wave cannot emerge before the incident wave enters the scattering region. In this inequality, ϕ is the potential scattering phase shift, k the wave number, and R the radius of the hard sphere. The energy variation of the $J_B=1^-$ potential phase shift, as revealed in the scattering amplitude diagram of $f(1)$ versus $g(1)$, violates this inequality by about a factor of 10 between 887 and 1220 kev. However, it is felt that this violation is not

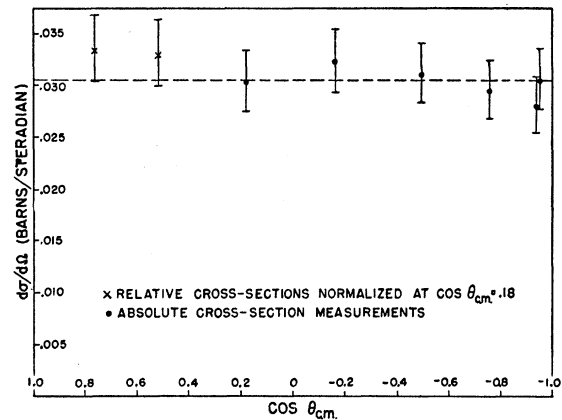


FIG. 21. The differential cross section for $Be^9(p,d)$ at $E_1=333$ kev. (Note suppressed zero of ordinate scale.)

sufficient to cast very strong doubt on the validity of the analysis, for the following reason.

The variation with energy of the s -wave $J_B=1$ potential phase shift is determined essentially by the 887- and 1084-kev theoretically deduced phases, since all other phases can be varied over a rather large range without disturbing the theoretical fitting to any great extent. The reasons why the 887- and 1084-kev fitting parameters cannot be varied greatly are that the 1084-kev fit comes from the narrow level analysis which is rather sensitive to $f(1)$ and $g(1)$, and the 887-kev analysis occurs in a region where the elastic scattering cross section is nearly equal to the Coulomb cross section. This means that at 887 kev the theoretical $[(d\sigma/d\Omega)/(d\sigma_R/d\Omega)]-1$ is a small number obtained from differences of large numbers, and the analysis is extremely sensitive to the choice of the fitting parameters. Inclusion of another p -wave amplitude to explain the reaction cross-section angular anisotropy around

¹¹ E. P. Wigner, Phys. Rev. **98**, 145 (1955).

800 keV would thus mainly affect the 887-keV analysis without disturbing the other angular distributions greatly. This in turn might move the $J_B=1^-$ fitting parameters at 887 keV in such a direction as to decrease $d\phi/dk$ by a large factor.

This scattering amplitude diagram plot of $f(2)$ versus $g(2)$ exhibits segments of two counterclockwise circles whose near tangency with the unit circle indicates little or no nonresonance reaction cross section in the $J_B=2^-$ s -wave channel. The amount of rotation of the centers of the two circles from the real axis being indefinite but fairly small, there is a lesser amount of potential scattering evidenced in the $J_B=2^-$ channel than in the $J_B=1^-$ channel. The resonance energies of the two states, corresponding to rotations through half the resonance circles, are about 998 and 1330 keV, respectively. The ratio of proton to total width is given by the radii of the two circles as $\Gamma_p/\Gamma=0.65\pm 0.15$ for both states. The total widths of the two states obtained from the low-energy side of the 998-keV resonance

TABLE I. Properties of the states of B^{10} reached by Be^9+p .

Properties determined from $Be^9(p,p)$			Properties determined from $Be^9(p,d)$; $Be^9(p,\alpha)$; $Be^9(p,\gamma)$		
E_r (keV)	J_r parity	Widths	E_r (keV)	J_r parity	Widths
330	$1^-, 2^-$	$\frac{\Gamma_p(330)}{\Gamma(330)} \sim \begin{cases} 0.18 & \text{if } J_B=2 \\ 0.30 & \text{if } J_B=1 \end{cases}$	336	1^-	$\frac{1}{3}\theta_p^2 \sim 0.5$ $\frac{1}{3}\theta_d^2 \sim 0.4$ $\frac{1}{3}\theta_\alpha^2 \sim 0.05$
980	2^+	$\Gamma_p/\Gamma \sim 0.9$ ($\theta_p^2 \sim 0.07$)	993	2^-	$\Gamma = 88$ keV $\Gamma_r = 23$ eV
998	2^-	$\Gamma_p/\Gamma = 0.65 \pm 0.15$ $\Gamma = 150 \pm 50$ keV $\frac{1}{3}\theta_p^2 \sim 0.02$	1085 ± 2	0	$\Gamma_\gamma = 6.0$ eV
1084 ± 2	0^+	$\Gamma = 3$ keV			
1330	2^-	$\Gamma_p/\Gamma = 0.65 \pm 0.15$ $\Gamma = 400 \pm 100$ keV $\frac{1}{3}\theta_p^2 \sim 0.05$			

circle, the high-energy side of the 1330-keV resonance circle, and Eq. (4), are $\Gamma(998)=150\pm 50$ keV and $\Gamma(1330)=400\pm 100$ keV. The reduced proton widths of the 998 and 1330-keV states are respectively about 2% and 5% of the single-particle limit.

Since much information on the states of B^{10} is obtained from the elastic scattering analysis assuming a 2^+ p -wave state at 980 keV, it is interesting to compare the conclusions of this analysis with those obtained from a study of gamma rays and reaction products from the proton bombardment of beryllium.

Gamma-ray transitions to the ground state from the s -wave state near 1 MeV are electric dipole while those from the p -wave state are magnetic dipole. If $\alpha_1^2=1$, the p -wave state is formed only by channel spin one and the two types of gamma rays do not interfere. The electric dipole gammas are isotropic while the magnetic dipole gammas have the angular distribution $1+0.167 \sin^2\theta$. Thus, the combination of s -wave and p -wave $J_B=2$ states near 1 MeV can lead to the observed angular distribution $1+(0.10\pm 0.03) \sin^2\theta$, with approx-

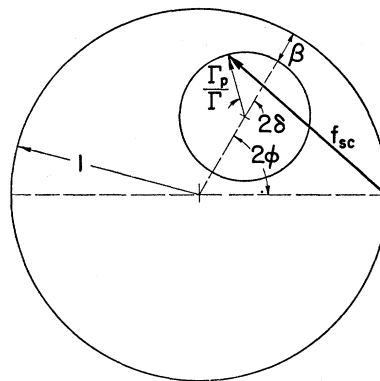
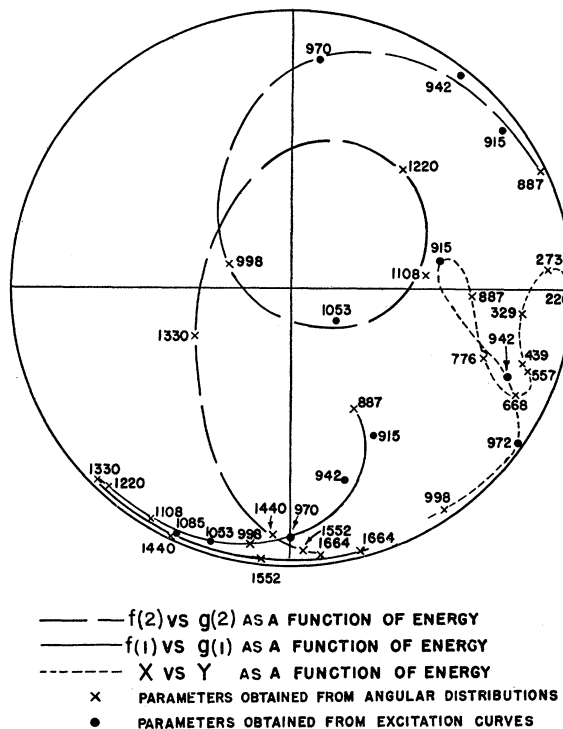


FIG. 22. Scattering amplitude diagram for one-level resonant scattering with potential scattering and resonant and nonresonant reactions.

priate and reasonable choices of the partial gamma widths.

Additional experimental information has been obtained by Devons¹² from a study of the angular correlation of internal conversion pairs, a study whose theoretical interpretation gives the strength of the various multipole orders involved in the gamma transition. From the bombardment of 50- to 100-keV thick beryllium foils with protons of energies between 950 and 1050 keV, Devons deduces the existence of a

FIG. 23. S -wave scattering amplitude diagrams obtained from theoretical fits of the experimental elastic scattering data.

¹² S. Devons and G. Goldring, Proc. Phys. Soc. (London), A67, 413 (1954).

mixed $E1$ and $E3$ or $M2$ transition to the ground state, with the $E1$ gamma width being about 3% of that predicted by the single-particle model. However, the $E3$ or $M2$ width comes out about 10^3 times larger than that predicted by either the single particle or liquid drop models. This theoretically impossible conclusion is obviated under the assumptions of a p -wave 2^+ state at 980 keV and an s -wave 2^- state at 998 keV, since the resultant $M1$ and $E1$ transitions to the ground state will lead to roughly the experimental angular correlation of internal conversion pairs for gamma widths within the single-particle model limit.¹³

The $\text{Be}^9(p,d)$ and $\text{Be}^9(p,\alpha)$ experimental determinations below 1 MeV provide much insight into the states of B^{10} . The principal experimental facts are that the total reaction cross sections are peaked near 940 keV and exhibit angular anisotropies that indicate an interference between states of opposite parity that is large in the region between 500 keV and 1 MeV. These behaviors are qualitatively partially understood in terms of the elastic scattering analysis, but their quantitative theoretical interpretation must depend on more thorough experimental data and analysis.

The qualitative understanding of the total reaction cross-section peaking about 50 keV below the 998-keV proton or gamma-ray resonance energy follows from the assumption that the reaction products are produced by the $J_B=2^-$ level and the realization that there are two overlapping states of the same spin and parity in B^{10} , the 998- and 1330-keV 2^- levels. Under such circumstances it is possible for the total reaction cross section to peak at an energy different from the true resonance energy. It must be pointed out, however, that such a behavior is not predicted by the scattering amplitude diagram plot of $f(2)$ versus $g(2)$ which predicts that the s -wave reaction cross section will peak near one MeV.

The peaking of the $\cos\theta$ term in the reaction angular distributions near 1 MeV is explained by the presence of the 2^+ p -wave state if the assumption that $\alpha_1^2=1$ is relaxed somewhat to allow for the formation of this state through channel 2. The state can then interfere with the 2^- s -wave state which is only formed in channel 2.

The interference between states of opposite parity that exists down to 500 keV in the reaction product angular distributions cannot be understood in terms of

the states deduced from the elastic scattering experiment. It is plausible that a second p -wave state with a small proton width exists near 700 keV. Such a state might produce a negligible effect in elastic scattering but could cause interference in the reaction product angular distributions. The test of this hypothesis should involve a non-proton-induced reaction leading to this energy region in B^{10} . The only choice of a nuclear reaction satisfying these requirements is $\text{Li}^6+\alpha$. A study of the reaction products and elastic scattering produced under bombardment of Li^6 by alpha particles near 5 MeV might lead to a clarification of the theoretical situation of the states of B^{10} near 7.50 MeV.

It is seen that the assumption of a 2^+ p -wave state at 980 keV in the proton bombardment of beryllium explains the experimental elastic scattering data quantitatively, the gamma-ray data at least semi-quantitatively, and the reaction data qualitatively in part. It is thus of pertinent interest to inquire into some further experimental method of testing the hypothesis of the existence of such a state.

A plausible experimental test could be to study the polarization effects produced by the elastic scattering of 1-MeV protons by beryllium in a double-scattering experiment. Under the assumptions of only s -wave states and Coulomb scattering, no polarization will be produced, while the presence of a p -wave state in addition to the s -wave states results in a theoretically calculable amount of polarization. An experiment of this type is presently being designed.

As a final remark on the possible existence of a 2^+ state in B^{10} , it should be noted that in a recent article, Kurath¹⁴ applies an intermediate coupling scheme to B^{10} and theoretically deduces the energies of the first five even-parity states almost quantitatively. He also predicts the existence of a 2^+ state at almost exactly the same energy as that hypothesized from the theoretical analysis of the elastic scattering of protons by beryllium.

IV. ACKNOWLEDGMENTS

The author wishes to express his gratitude to Dr. W. A. Fowler, Dr. C. C. Lauritsen, and Dr. T. Lauritsen for suggesting the experiment and aiding in the collection of experimental data, and to Dr. R. F. Christy for the method of theoretical analysis of these data.

¹³ R. F. Christy (private communication).

¹⁴ D. Kurath, Phys. Rev. **101**, 216 (1956).